Military Technical College
Kobry El-Kobba,
Cairo, Egypt

11-th International Conference
on Aerospace Sciences &
Aviation Technology

A NEW APPROACH FOR MOVING TARGET DETECTION USING BARTLETT METHOD FOR SPECTRAL ESTIMATION

Abdel Rahman H. Elbardawiny*, Khairy A. Elbarbary*, and Fathy M. Ahmed*

ABSTRACT

Moving Target Detection (MTD) is an automated radar signal and data processing system, which is designed to improve the performance of radar systems in the presence of various forms of clutter. Consequently, it provides high probability of detection (P_d) for an acceptable probability of false alarm (P_{fa}). It employs coherent, linear Doppler filtering, adaptive thresholding and a fine ground clutter map to reject ground clutter, rain clutter, birds, and interference.

The current MTDs relay on the Fast Fourier Transform (FFT) of the total received data sequence to estimate the clutter power spectrum and consequently reduce or remove its effect on the detection performance. Direct FFT leads to high sidelobes level and requires a significant large computation time. The high level sidelobes increases the false alarm probability at the output of the Doppler filters bank. A solution for reducing the effect of spectral sidelobes is the utilization of window functions. However, this solution leads to widening the main spectral lobe and reduce the Doppler resolution. Also it increases the hardware complexity of the system.

In the present work, Bartlett method for spectral estimation which depends on dividing the received data sequence into a number, K, of nonoverlapping segments and averaging the calculated FFT for each segment over K, is applied in the MTD instead of the direct FFT for typical ground based radar. The proposed method enhances the target detection capabilities, by providing higher detection probabilities, lower false alarm rates and an additional gain of 7~10 dB in the improvement factor, in the presence of ground and weather clutter, compared to the traditional one. This is because the sidelobe levels obtained are very small in magnitude. This in turns facilitates the realization of the Doppler filters bank without using additional weighting.

The obtained performance can be achieved by applying the direct FFT with weighting function to the total received data sequence, which leads to a more hardware complexity and long time calculations compared to the proposed method. Computer simulation results are presented to support the superiority of the proposed technique.

* Egyptian Armed Forces

1. Introduction

The classical problem in radar signal processing is the detection of target in the presence of unwanted echoes called clutter. The clutter may arise due to the following:

- Reflections from fixed or slowly moving objects such as trees, vegetations and man made structures.
- Storm clouds and precipitations.
- Migration flocks of birds.

It has been established that while ground clutter has a very narrow spectrum, at or near zero Doppler, the clutter due to bird returns is more widely spread in frequency with the center frequency being shifted noticeably away from the zero Doppler [1]. Tow techniques are available in filtering out the clutter; the conventional moving target indicator (MTI) and an improved technique called the moving target detection (MTD).

MTD has been proposed as an improved radar signal processor because of the MTI's inability to detect targets in the presence of weather clutters as well as migration bird flocks. MTD achieves this improved performance because of the extensive use of Doppler filtering schemes, adaptive thresholding and fine ground clutter map. It has been shown that MTD meets the requirements of blind speed elimination and good sub-weather visibility while observing good probability of detection (P_d) and probability of false alarm (P_{fa}) [2,3].

Three MTD schemes are presently in use, namely MTD-I, MTD-II, and MTD-III. While MTD-I uses fast Fourier transform (FFT) as a Doppler filters bank, MTD-II, and MTD-III employs a seven-point and an eight-point finite impulse response (FIR) filter, respectively, as the Doppler filters bank [4,5]. In this paper only the MTD-I scheme, generally, we'll call it MTD, is considered because of its widespread usage as well as its simplicity [6].

The heart of the MTD radar digital signal processor is a bank of Doppler filters designed using FFT algorithm of length ideally equal to the number of the returned pulses during each illumination time. For high pulse repetition frequency (HPRF) radar, this number is high, leading to a long time calculations and great complexity in hardware implementation. To reduce calculation time and hardware complexity, only part of these pulses is processed at the expense of reduction in performance. The proposed technique using Bartlett method (MTD-B) achieves the reduction of hardware complexity and time calculations with keeping a good performance as if we process the total pulses in the received observation.

The work described in this paper was entirely simulation-based using Matlab 6.5 package. The composite radar video signal has been simulated using the method proposed in [7]. The performance of the two systems, the traditional MTD (FFT-based) and the proposed MTD-B (Bartlett-based), has been compared from the viewpoint of probability of detection, probability of false alarm, and the improvement factor (IF). Typical HPRF radar was chosen for the simulation study [6].

The rest of this paper is organized as follows; section 2 describes the MTD operation and explains briefly the idea of operation of each block in the system including the use of FFT or the proposed Bartlett method. Section 3 discusses the performance measures used in simulation. Section 4 presents the method used to simulate composite radar video signal. Section 5 shows the results of simulation and discussions. Finally section 6 contains the conclusion and suggested future work.

2. MTD Operation

The coverage area in a modern radar system can be depicted as shown in Fig. 1 [1]. The radar space is divided into a number of range-azimuth (RA) cells. The entire range is divided into 'P' range cells and the azimuth into 'M' cells. Since the antenna has to spend a certain time in each of these 'M' azimuth rays, a fixed number of pulses is always returned from each of these 'P' rang cells. This batch of pulses from each RA cell is called the coherent processing interval (CPI), which is processed by the MTD. For the typical HPRF radar considered, the number of returned pulses in each range azimuth cell is 133 pulses [6]. These returned pulses must be fastly processed, to decide whether the returned signal is due to presence of target or clutter and noise alone. Usually, targets are distinguished from clutter by their relative Doppler shifts in the returned signal. This is achieved by implementing either pulse Doppler processing, moving target indicator (MTI), or MTD. In this work, we are interested in MTD whose block diagram, FFT-based and the proposed Bartlett-based, is shown in Fig. 2.

The received radar signal, after converting into intermediate frequency (IF), is passed through a band pass filter (BPF) having the center frequency of the filter as IF and bandwidth equal to the inverse of the pulse width [8]. The signal from the BPF is then fed to a synchronous detector to drive the in-phase and quadrature phase signals (I, and Q respectively). The input to the MTD processor is the discrete I and Q samples. Each block in the MTD structure of Fig. 2 is briefly explained in the following sections.

2.1. The three pulse canceller

The delay line canceller acts as a filter, which rejects the returned signal from stationary clutter. Consequently, the DC components of clutter spectrum are removed. The structure of the double delay line canceller is shown in Fig. 3. A double delay line canceller arranged in a proper configuration acts as a three-pulse canceller whose output, y_n, is related to the input, x_n, by the difference equation given by:

$$y_n = x_n - 2x_{n-1} + x_{n-2} \tag{1}$$

Where x_n represents the n^{th} complex input sample combining both I and Q outputs of the synchronous detector. As the first two output pulses from the three-pulse canceller are meaningless, only the last (CPI-2) of the CPI pulses are passed into the subsequent blocks.

2.2. The zero velocity filter (ZVF)

The function of the zero velocity filter is the detection of any target, at low velocities or moves at a tangential trajectory to the antenna pattern, whose returns exceeds the level of clutter in that particular cell. The algorithm used is such that it accumulates the I and Q signals for the first CPI/2 input signals and takes the magnitude of the results. This process is repeated for the second CPI/2 signals. The two magnitudes are then added to form a number indicating the strength of the zero velocity component of the signal. The zero velocity strength of a particular cell can be obtained by [1].

$$Z = \frac{1}{2}\left\{ \left| \sum_{k=1}^{CPI/2} [I(k) + jQ(k)] \right| + \left| \sum_{k=(CPI/2)+1}^{CPI} [I(k) + jQ(k)] \right| \right\} \quad (2)$$

2.3. Doppler Filters Bank

2.3.1. Using FFT (MTD-I)

The heart of the MTD signal processor is a bank of Doppler filters designed for better clutter rejection and coherent integration of the pulses. For a CPI length of 130 out of 133, this Doppler filters bank is realized for MTD-I by FFT algorithm of length 128. The fast Fourier transform is built based on the discrete Fourier transform given by:

$$Y(m) = \sum_{n=0}^{N-1} y(n) \exp(-j \frac{2\pi mn}{N}) \quad (3)$$

Where m, n = 0,1 2,.....,N-1. Such that $y(n)$ is the input data sequence, N is the length of this sequence which equal to 128.

It has been established that the standard radix-2 FFT takes $(N/2)log_2(N)$ complex multiplications, and $(N)log_2(N)$ *complex additions* [1]. For N=128, the total complex operation is 1344. For simplicity, of calculation and hardware implementation, a CPI length of 34 is chosen, and the length of the FFT algorithm is 32, leads to a number of 304 complex operations.

The 32 pulses output data from the three-pulse canceller is fed to the Doppler filters bank. The three-pulse canceller, followed by the Doppler filters bank, eliminates the zero velocity clutter (stationary clutter) and generates 32 overlapping filters covering the total Doppler interval (because of using complex signal instead of real signal). The detection here takes place based on frequency domain. The peak of the Doppler filters bank output is detected after proper thresholding declaring the presence of target. The location of this peak declares the corresponding Doppler frequency.

2.3.2. Using Bartlett Method (MTD-B)

In the proposed technique using Bartlett method, the CPI length of 130 out of 133 is chosen. Consequently, the useful signal length after the three-pulse canceller is 128.

This data sequence is divided into four equal nonoverlapping segments. The segment length is 32 samples. For each segment, the FFT is computed. The magnitude of the Bartlett spectral components is obtained by averaging the FFT, previously computed, over the four segments. Computation of this method is described by the following equations:

$$\overline{Y}(m) = \frac{1}{K}\left|\sum_{k=0}^{K-1} Y(m)\right| \tag{4}$$

Where,

$$Y(m) = \sum_{n=kL}^{(k+1)L-1} y(n)\exp(-j\frac{2\pi mn}{L}) \qquad k=0,1,2,3 \quad ; \; 0 \le m \le L-1 \tag{5}$$

Such that,

$\overline{Y}(m)$ is the Bartlett spectral component at any frequency bin, m.
$Y(m)$ is the discrete Fourier transform of the segment data sequence $y(n)$.
K is the number of data segments, and equal to 4.
L is the segment length, and equal to 32.

Using this method, we need only to implement the FFT hardware of length 32 one time while utilizing the total 128 data points. This leads to a reduction in hardware complexity compared to the direct computation of the FFT of length 128, which is the first goal of this method.

Because of the averaging procedure on the computed FFT of all segments, a reduction of the spectral variation is obtained, which is the second goal.

Noise is a random process, unlike target signal, and the addition performed in equation 4 takes place for complex values, not magnitude. So, a reduction of the sidelobes level due to noise is obtained compared to the target signal, which is the third goal of this technique. A further reduction in hardware complexity is obtained by removing the additional weighting applied after the Doppler filters bank in the traditional MTD-I (FFT-based) if we apply the MTD-B (Bartlett-based).

Simulation of the performance of the proposed MTD-B (Bartlett-based) compared to the traditional MTD-I (FFT-based) is introduced in section 4 with more discussion to verify the superiority of the proposed technique.

2.4. Weighting

Following the FFT filter bank, weighting is applied to the signal in the frequency domain to reduce the effect of leakage present at the output of the FFT. The

weighting algorithm, which uses a Hamming weighting function, can be represented as follows [1,6]:

$$y_m = y_m - 0.25\,(y_{m-1} + y_{m+1}) \tag{6}$$

Where, y_m represents the m^{th} filter output. This algorithm is equivalent to Hamming weighting function applied at the input of the FFT [1,6]

2.5. Clutter map

The function of this block is to establish a threshold for the ZVF output. The signal generated from this clutter map will be used to detect the targets on crossing trajectories with zero Doppler shifts. This function is achieved as discussed below.

In each range cell of the ground clutter map, the average value of the output of the ZVF for the past scans is stored. The map is updated in a recursive manner as follows [1,6]:

$$M_m = (1-\alpha)\,M_{m-1} + \alpha\ Z_m \tag{7}$$

Where M_m is the new update of the cell stored in the map, M_{m-1} is the previous value stored in that cell, and Z_m is the present output of the ZVF. For the MTD considered, the value of α chosen is 1/8 [1,6].

2.6. Thresholding

Separate thresholds are established to each filter output. The threshold for the ZVF is established by the output of the clutter map multiplied by a constant [1]. Since weather clutter is somewhat time varying and spread in rang over several cells, thresholding of any nonzero velocity filter is done depending on the average returns of that filter leading to a form of constant false alarm rate (CFAR). The structure of a cell average (CA) CFAR is shown in Fig.4. The window length chosen for CFAR is 16 range cells [1,6].

This means that the filter output of the previous 8-cells, and 8-cells after the cell of interest, are averaged according to the following equation:

$$T_{tc} = \frac{1}{16}\left[\sum_{k=tc-8}^{tc-1} y_k + \sum_{k=tc+1}^{tc+8} y_k\right] \tag{8}$$

Here, T_{tc} represents the threshold value of the cell of interest, tc, and y_k values are the past 8-cells and the 8-cells after the cell of interest. The more remarkable property of a CFAR is the possibility to set the detection threshold to guarantee a pre-assigned false alarm probability, P_{fa}, independent of the disturbing reasons [9]. The Doppler returns which cross the threshold will be reported as target present;

otherwise it is taken as target absent. If the Doppler returns cross the threshold when there is no target, it is called false alarm. Different CFAR schemes like greatest-of (GO) CFAR, smallest-of (SO) CFAR, or order statistic (OS) CFAR may be used instead of the cell average (CA) one shown in Fig.4. This depends on the design requirements.

3. Performance Measures

The performance of the two systems, the traditional MTD-I and the proposed MTD-P has been compared from the viewpoint of probability of detection, probability of false alarm, and the improvement factor (IF). The improvement factor is defined, for MTD, as the ratio of the *SCNR* at the filters bank output to the *SCNR* at the filters bank input, averaged uniformly across all the target Doppler frequencies. The algorithm used is given by [6]:

$$IF = \frac{1}{N} \frac{\sum_{n=1}^{32} SCNR_O(n)}{\sum_{n=1}^{32} SCNR_I(n)} \qquad (9)$$

Where $SCNR_O(n)$ is the signal-to-clutter+noise-ratio at the output of filter number n, $SCNR_I(n)$ is the signal-to-clutter-noise-ratio at the input of the MTI for a normalized target Doppler shift of $n/32$, and N is the total number of the output taps of the Doppler filters bank.

4. Computer Simulations

4.1. simulation of composite radar video signal

For the purpose of simulating MTI-I and the proposed MTD-B schemes, a composite radar video signal is generated using the simulation model outlined in [7]. The radar signal developed is capable of simulating a composite radar environment with ground and weather clutter along with the receiver thermal noise and target returns. Various parameters of the clutter, namely, spectral width, clutter to noise ratio (CNR) and Doppler frequency can be chosen independently.

According to Barlow [1], the power spectra due to various sources of radar clutter may be approximated by Gaussian spectra at the Doppler frequency f_d and is given by:

$$S(f) = S(\quad) \exp((\quad f - f_d)^2 / 2\sigma_f^2) \qquad (10)$$

Where σ_f^2 is the spectral width.

A typical HPRF radar with PRF = 4000 Hz, and antenna scanning rate of 60 deg./sec with beam width of 2 deg. is used in simulation. These values resulted in a number of 133 hits in every illumination time. The CPI length used for the MTD-I is chosen to be 34 out of 133 [6]. For the purpose of performance evaluation, the performance of the MTD-I is also simulated for a CPI length of 130. The CPI length for the proposed MTD-B is chosen to be 130 out of 133.

The ground clutter simulated is Log-Normal distribution with zero mean Doppler and spectral width of 50 Hz. The weather clutter simulated is Rayleigh distribution with mean Doppler frequency of 500 Hz, and 250 Hz spectral width. The thermal noise simulated is additive white Gaussian with zero mean and variance σ^2.

4.2. Detection Performance

The setup procedure for measuring the detection performance is valid for both MTD-I and the proposed MTD-B schemes. Target signal is added to the clutter with a desired Signal-to-Clutter+Noise-Ratio (SCNR). The total normalized Doppler frequency is divided into 32 intervals. The number of range cells examined for each filter is chosen to be 32. Also the target is introduced with a known Doppler frequency in one of the range cells with a uniform probability of 1/32.

As a first step in simulation, the probability of false alarm, P_{fa}, after the CFAR block is computed for different threshold gains at various Clutter-to-Noise-Ratios (CNR). The results obtained are shown in Figs. 5a and b for threshold gains of 2 and 3 respectively corresponding to MTD-I and the proposed MTD-B. It is obvious that both schemes give the same P_{fa} at light clutter (CNRs < 0 dB). For heavy clutter (CNRs > 0 dB), the proposed MTD-B outperforms that of the traditional MTD-I because of the low spectral variation and side lobe levels obtained. The reason that the P_{fa} in both schemes goes high as the CNR increases, more than o dB, is the application of CA-CFAR scheme which acts bad in the situation when the disturbing noise is nonhomogeneous (not Gaussian). We can overcome this problem by applying a greatest of (GO) CFAR scheme [11]. In our simulation, the lowest P_{fa}, which can be achieved, is 10^{-3} (32 filter tabs x 32 range cells).

The probability of detection, P_d, for the MTD-I and the proposed MTD-B is shown in Figs 6a and b at different SCNRs for threshold gains of 2 and 3 respectively. These figures show the superiority of the proposed technique over the traditional one. For example, at SCNR of -15 dB, CNR of 0 dB, threshed gain of 2, and P_{fa} of 0.057 for both detectors, the P_d was 70% for the proposed MTD-B and 20% for the traditional MTD-I.

Figs. 7a and b show tow plots for the detection probability of the MTD-I and the proposed MTD-B for different target Doppler shifts at CNR of -30dB and SCNR of -10 dB for a designed P_{fa} of 0.003 and 0.056 respectively. Both detectors give almost a steady performance over different Doppler shifts with the superiority of the proposed technique.

4.3. Improvement Factor

The improvement factor setup is also valid for both MTD-I and the proposed MTD-B. Initially clutter alone is fed to the MTD input and the output is collected for power computation just before the CFAR block. Later, target alone is introduced and a similar process is carried out. Target frequencies are selected such that it appears at the filter taps with a uniform probability of 1/32.

Fig.8a shows the improvement factor against target Doppler shifts for both MTD-I (32_FFT and 128_FFT) and the proposed MTD-B in case of presence of the simulated ground and weather clutter with the mentioned parameters along with the target. The effect ofweather clutter is slightly reducing the improvement factor for all schemes for target Doppler shifts lying in the clutter region. There is a little difference in IF between the proposed MTD-B and the MTD-I (128_FFT) in favor of the later. This difference is disappeared as the CNR decreases, as shown in Fig. 8b.

Figs. 9a and b show the improvement factor against the CNR and the SCNR respectively for the MTD-I and the proposed MTD-B. A gain of 7~10 dB in IF is achieved with the proposed MTD-B over the traditional MTD-I (32_FFT). This is because of the lower level and variance of the side lobes obtained by Bartlett method, which reduces the amount of clutter and noise power coming out of the filters bank, compared with the traditional FFT.

5. CONCLUSIONS

A novel scheme using Bartlett spectral estimation method is proposed for realizing moving target detection (MTD). The proposed technique, MTD-B (Bartlett-based), shows a superior performance over the traditional MTD-I (FFT-based) from the viewpoint of detection probability, false alarm rate, and the improvement factor in the presence of ground and weather clutter. This is achieved because the sidelobes obtained are very small in level and variance compared to the traditional one. Computer simulations were provided to support the superiority of the proposed technique. Investigation and further analysis for the following points may be taken into consideration:

- Choosing the number of data segments, K, or overlapping them.
- Changing target velocity (Doppler shift) during the illumination time.
- Comparison between the proposed MTD-B and that presented in [6], MTD-WVD, which depends on the computation of the Wigner-Ville Distribution (WVD) for the received data sequence to form the Doppler filters bank.
- Applying Bartlett method in the adaptive moving target detection (AMTD).

6. REFERENCES

[1] J. Giridhar, K. M. M. Prabhu, "Implementation of MTD-WVD on a TMS320C30 DSP Processor", Microprocessor and Microsystems 22, pp 1-12, (1998).

[2] C.EMuehe, "Moving Target Detector, an improved signal processor", Proc. Intl. Conf. AGARD 195, (1975).

[3] C. E. Muehe, "Advances in Radar Signal Processing", Presented at Electro, pp. 1-9, 25 May (1976).
[4] D. Karp, J. R. Anderson, "Moving Target Detector (MOD-II) Summary Report", MIT Lincoln Laboratory, Report No. ATC-95, (1981).
[5] Byron Edde, "Radar Principles. Technology and Applications", Prentice Hall PTR, Englewood Cliffs,NJ,(1993).
[6] P. Krishna Kumar, K.M.M. Prabhu "Simulation Studies of Moving Target Detection: a New Approach With Wigner-Ville Distribution", Proc. IEE, Radar, Sonar and Navigation, Vol. 144, No. 5 , pp. 259-265, (1997).
[7] Mitchell, R.L. "Radar Signal Simulation", Artech House, (1976).
[8] Merril I. Skolnik, "Introduction to radar systems (3rd ed.)", McGraw-Hill, (2001).
[9] A. De Maio, G. Foglia, E. Conte., "CFAR Behavior of Adaptive Detectors: An Experimental Analysis", The proceeding of IEEE Radar conference, (2004).
[10] Barlow, E.J " Doppler Radar ", Proc. IRE- 37, pp. 340-355, (1949).
[11] Rohling H., "Radar CFAR Thresholding in Clutter and Multiple Target Situations", IEEE Trans., AES-19, pp608-621, (1983).

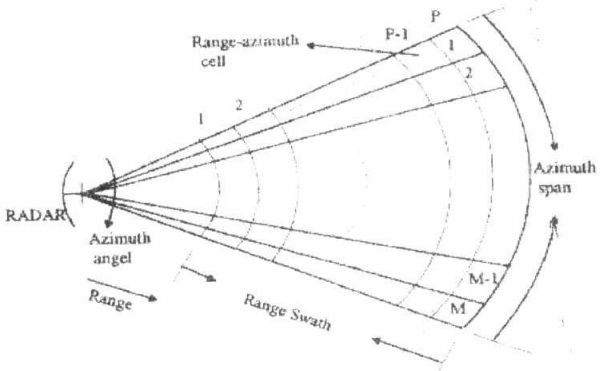

Fig.1. Modern radar operating environment

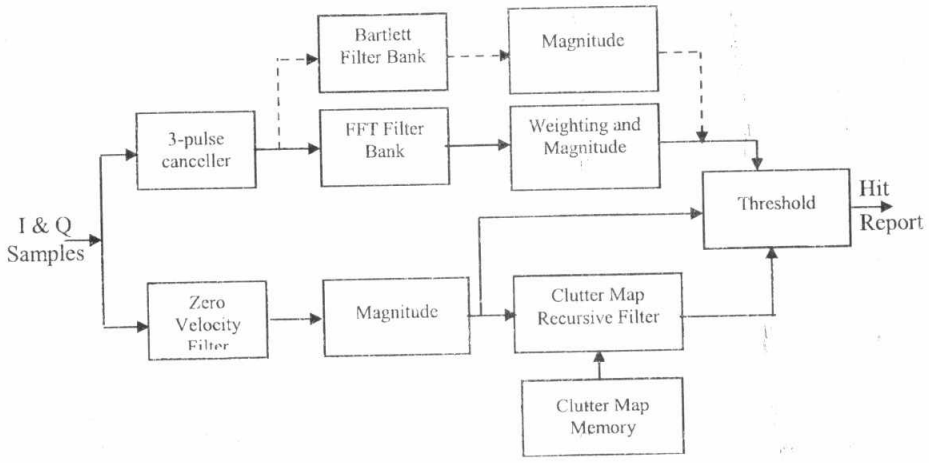

Fig.2. Block diagram of the MTD (— MTD-I , ····· MTD-B)

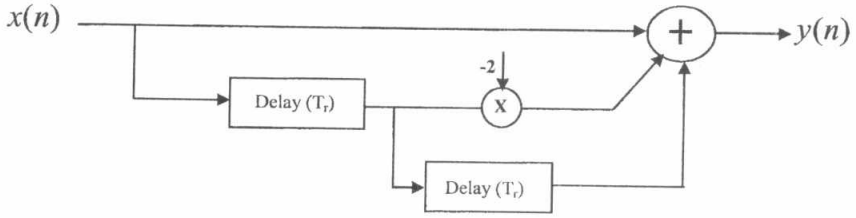

Fig.3. structure of the three-pulse canceller

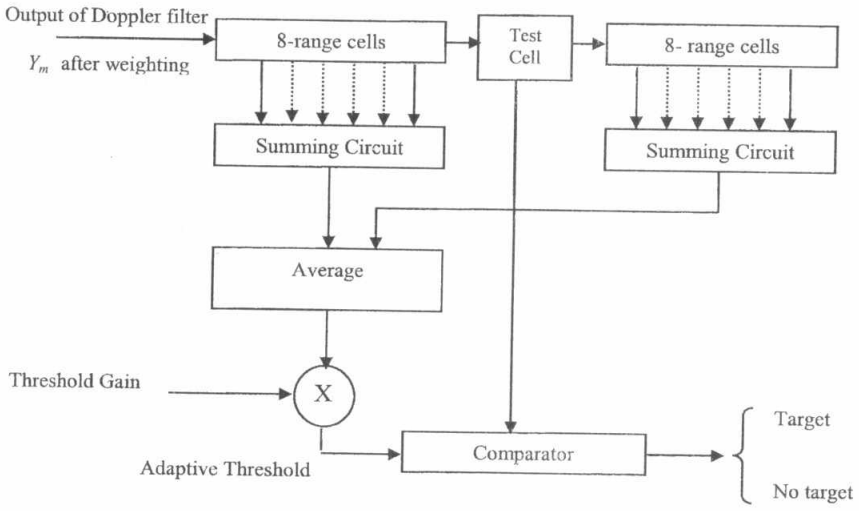

Fig.4. CA-CFAR scheme used for each output of the nonzero weighted Doppler filters bank

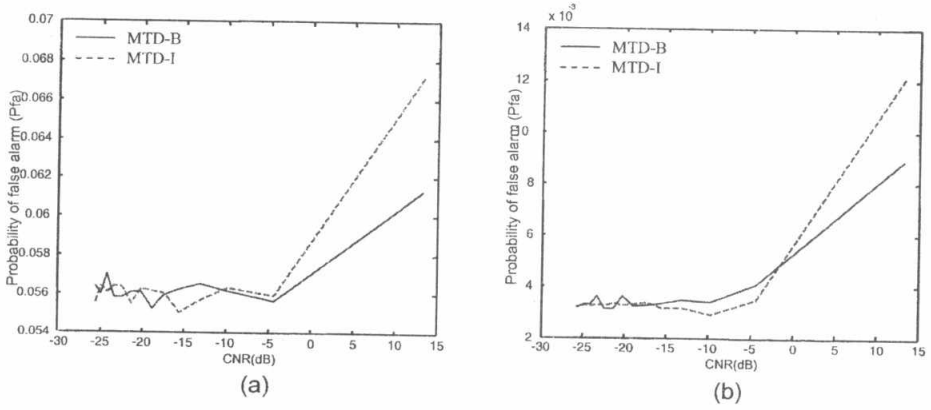

Fig.5. Probability of false alarm, P_{fa}, of MTD-I and MTD-B against CNRs
a- For threshold gain = 2
b- For threshold gain = 3

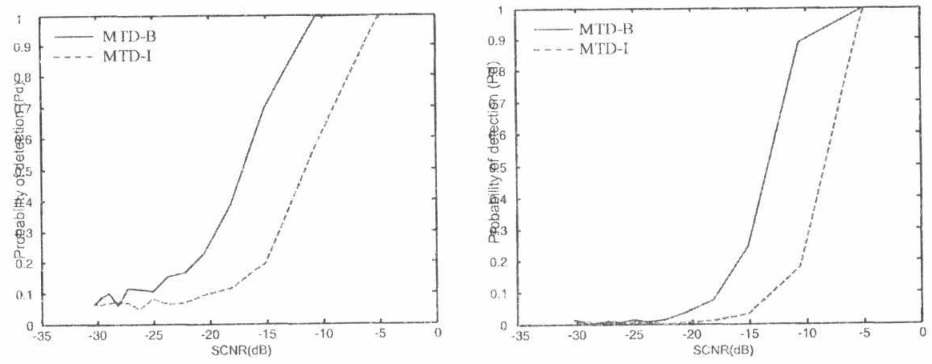

Fig.6. Probability of detection, P_d, of MTD-I and MTD-B against SCNRs

a- For threshold gain = 2
b- For threshold gain = 3

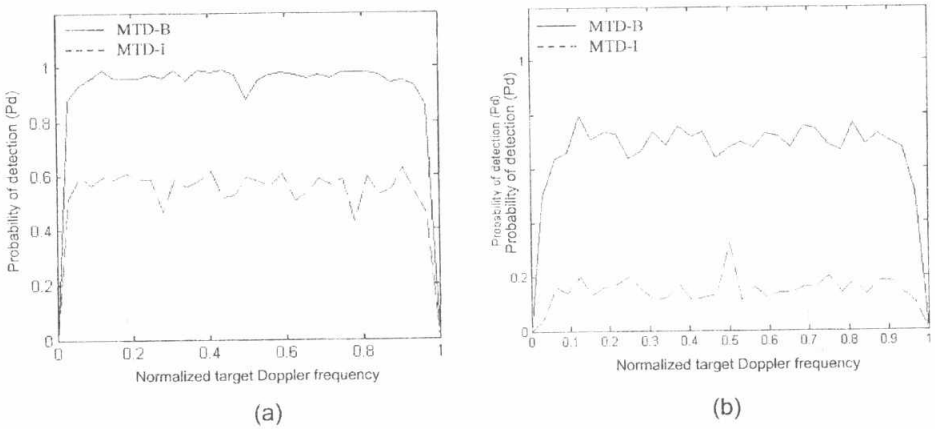

Fig.7. Probability of detection, P_d, of MTD-I and MTD-B against Doppler shifts, SCNR= -10dB,, and CNR=-30dB

a- For threshold gain = 2
b- For threshold gain = 3

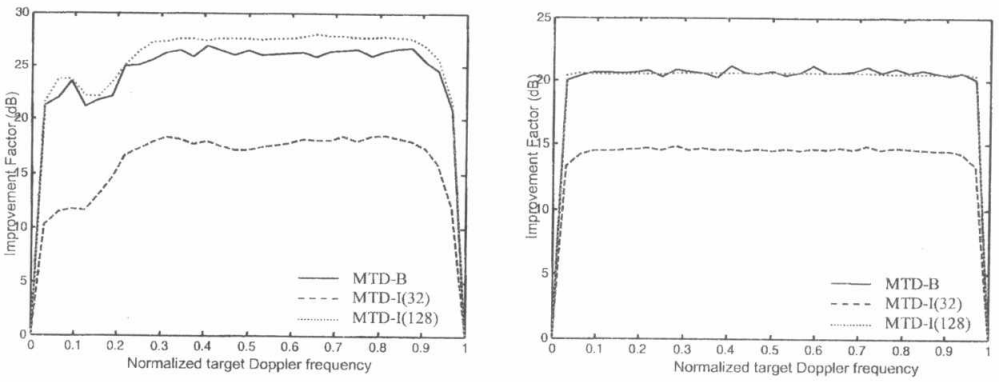

Fig.8. Improvement factor, IF, of MTD-I and MTD-B against normalized Doppler shifts

a- SCNR =-10dB, and CNR =10dB
b- SCNR =0dB, CNR =-30dB

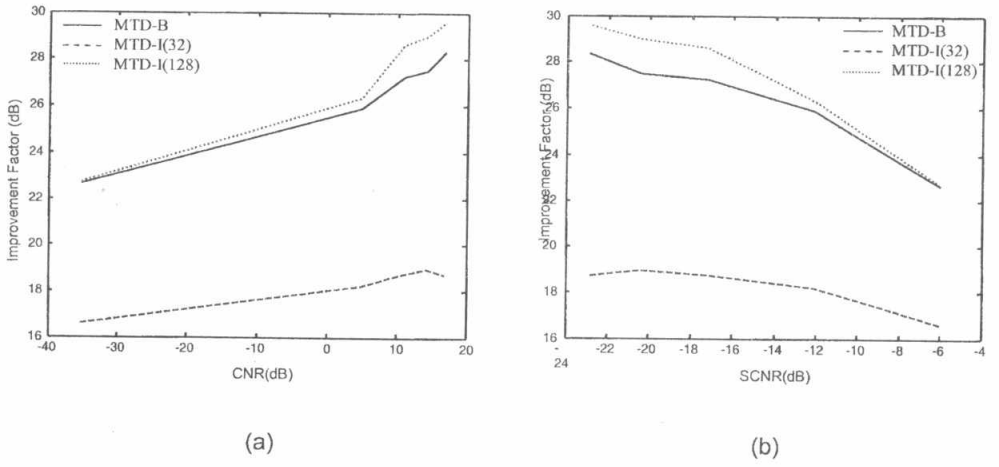

Fig.9. Improvement factor, IF, of MTD-I and MTD-B

a- Against CNRs
b- Against SCNRs

IMAGE PROCESSING

CONTENTS